

# Optically equalized 10 Gb/s NRZ digital burst-mode receiver for dynamic optical networks

Benn C. Thomsen, Benjamin J. Puttnam and Polina Bayvel

*Optical Networks Group, Electronic and Electrical Engineering Department, University College London, London, WC1E 7JE, United Kingdom.*

[bthomsen@ee.ucl.ac.uk](mailto:bthomsen@ee.ucl.ac.uk), [bputtnam@ee.ucl.ac.uk](mailto:bputtnam@ee.ucl.ac.uk), [pbayvel@ee.ucl.ac.uk](mailto:pbayvel@ee.ucl.ac.uk)

**Abstract:** A 10Gb/s NRZ burst-mode optical receiver suitable for receiving asynchronous bursts with power variations of up to 7 dB is presented. The digital burst mode receiver is based on a standard AC-coupled photodiode followed by asynchronous analogue to digital conversion at 20 GS/s. Symbol timing, amplitude and baseline wander corrections are implemented in digital signal processing without the need for additional linecoding, such as 8B10B, and special AC-coupling schemes. It is assumed that G.709 framing together with enhanced FEC is used therefore the receiver is characterized using a pre-eFEC BER of  $10^{-3}$  at an input OSNR of 10 dB. We show that the addition of an electronically controlled SOA for optical power equalization before the receiver extends the burst-to-burst dynamic range from the 7 dB provided by the digital receiver alone to 16.5 dB. The large dynamic range, low overhead, and burst length versatility make this type of receiver ideal for applications in both synchronous and asynchronous dynamic network architectures with burst timescales ranging from nanoseconds through to continuous data.

©2007 Optical Society of America

**OCIS codes:** (060.2380) Fiber Optics Sources and Detectors; (060.2330) Fiber Optics Communications; (230.5160) Photodetectors.

---

## References and links

1. P. Bayvel and M. Düser, "Optical burst switching: research and applications," Optical Fiber Communications Conference, FO1, 22-27, (2004).
2. Y. Ota and R. G. Swartz, "Burst-mode compatible optical receiver with a large dynamic range," IEEE J. Lightwave Technol., **8**, 1897-1903, (1990).
3. NRZ Bandwidth – LF Cutoff and Baseline Wander, Maxim inc. application note HFAN-09.0.4, <http://pdfserv.maxim-ic.com/en/an/4hfan904.pdf>
4. C. Su, L-K. Chen and K-W. Cheung, "Theory of burst-mode receiver and its applications in optical multi-access networks," IEEE J. Lightwave Technol., **15**, 590-606, (1997).
5. C. Su, L. K. Chen, K. W. Cheung, "BER performance of digital optical burst-mode receiver in TDMA all optical multiaccess network," IEEE Photon. Technol. Lett., **7**, 132-134, (1995).
6. P. Ossieur, "A 1.25-Gb/s burst mode receiver for GPON applications," IEEE, Journal of Solid-State Circuits, **40**, 1180-1189, (2005).
7. A. Dupas, B. Lavigne, W. Lautenschlaeger and S. Schabel, "10 Gbit/s RZ asynchronous packet mode receiver with high input power dynamic for future optical packet switching systems," Photonics in switching, Monterey USA, (2001).
8. M. Duelk et al., "Fast packet routing in a 2.5Tb/s optical switch fabric with 40Gb/s duobinary signals at 0.8b/s/Hz spectral efficiency," Optical Fiber Communications Conference, PD8, (2003).
9. F. M. Gardner, "Interpolation in digital modems – Part I: Fundamentals," IEEE Trans. Commun., **41**, 501-507, (1993).
10. B. C. Thomsen, B. J. Puttnam and P. Bayvel, "10 Gb/s AC-Coupled Digital Burst-Mode Optical Receiver," Optical Fiber Communication Conference, OThK5, (2007).
11. H. Wessing, B. Sorensen, B. Lavigne, E. Balmefrezol and O. Leclerc, "Combining control electronics with SOA to equalize packet-to-packet power variations for optical 3R regeneration in optical networks at 10 Gbit/s," Optical Fiber Communication Conference, OFC04, WD2, (2004).
12. S. J. Lee, "A new non-data-aided feedforward symbol timing estimator using two samples per symbol," Comms. Lett., **6**, 205-207, (2002).
13. J. H. Baek, J. H. Hong, M. H. Sunwoo and K. U. Kim, "Efficient digital baseline wander algorithm and its architecture for fast ethernet," IEEE SIPS, (2004).

14. M. Kawai, H. Watanabe, T. Ohtsuka and K. Yamaguchi, "Smart optical receiver with automatic decision threshold setting and retiming phase alignment," *IEEE J. Lightwave Technol.*, **7**, 1634-1640, (1989).
  15. V. J. Mazurczyk, R. M. Kimball and S. M. Abbott, "Using optical noise loading to estimate margin in optical amplifier systems," *Optical Fiber Communication Conference, OFC97*, TuP5, 85, (1997).
  16. N. S. Bergano, F. W. Kerfoot and C. R. Davidson, "Margin measurements in optical amplifier system," *IEEE Photon. Technol. Lett.*, **5**, 304-306, (1993).
  17. P. J. Winzer, et al., "10-Gb/s upgrade of bidirectional CWDM systems using electronic equalization and FEC," *IEEE J. Lightwave Technol.*, **23**, 203-210, (2005).
  18. C. Eldering, "Theoretical determination of sensitivity penalty for burst mode fiber optic receivers," *IEEE J. Lightwave Technol.*, **11**, 2145-2149, (1993).
  19. E. T. Aw, T. Lin, A. Wonfor, M. Glick, K. A. Williams, R. V. Penty and I. H. White, "Layered Control to Enable Large Scale SOA Switch Fabric," *European Conference on Optical Communications*, Th1.2.5, (2006).
- 

## 1. Introduction

Optical burst/packet (OBS/OPS) switching will be a key technology in next generation dynamically reconfigurable optical networks, that are able to adapt in response to changing traffic demand [1], and passive optical networks (PON) [2]. These networks require an optical receiver that is able to accurately recover the timing information and data from asynchronous optical bursts that exhibit large power fluctuations between them.

Conventional high bit-rate receivers are based on analogue designs that utilize an AC-coupled photodiode and transimpedance amplification stage. This is followed by clock recovery to track the slowly varying changes in the data arrival time and, thus, determine the optimum time at which the decision circuit samples the signal to recover the data. The use of AC-coupling significantly simplifies the design of the electrical amplifier and allows the threshold to be fixed. However, there are two major problems with using a conventional ac-coupled receiver for optical bursts. Firstly, the guard bands and power variations between bursts can lead to large DC offsets across the burst, called base line wander (BLW), that prevent setting the decision threshold at zero [3]. Secondly, the acquisition time of the clock recovery needs to be much faster as the symbol clock phase will vary both on a burst-by-burst basis and as well as within the burst [4].

Previous burst-mode receiver (BMR) implementations have solved the BLW problem either by using a DC-coupled receiver [2] or by utilizing line-coding [5]. DC-coupled burst mode receivers operating at 1.25 Gb/s have reported clock locking times of 25 ns and burst-to-burst dynamic ranges of 23.8 dB [6], however, this approach is yet to be reported at 10 Gb/s as it is complex and expensive to implement at higher bit-rates. Line-coding such as 8B10B reduces the low frequency data components allowing for a short AC-coupling time constant and enables the receiver to quickly adapt to variations in the optical power between bursts at the expense of an increased coding overhead (20% with 8B10B linecoding) that cannot be reduced by increasing the burst length. Such a burst mode receiver designed for 10 Gb/s return-to-zero formats demonstrated clock acquisition times as low as 2-3 ns with a dynamic range of 10 dB [7]. Similar burst mode receivers operating at 40 Gb/s have shown acquisition times as short as 15 ns [8].

Here we describe a 10 Gb/s Non-Return-to-Zero (NRZ) digital burst-mode receiver (DBMRx) that uses a conventional AC-coupled photodiode and transimpedance amplifier and does not require any line coding. The receiver uses a 20 GS/s analogue-to-digital converter (ADC) to asynchronously sample the output of the photodiode and performs the symbol timing and data recovery in the digital domain. This implementation is analogous to the digital modems that are already prevalent in wireline applications [9]. In this work the receiver operation is characterised at a reference BER of  $10^{-3}$ , where it is assumed that enhanced forward error correction (eFEC) requiring a 7.14% overhead will be used. The only additional fixed overheads in this scheme are the 32-bit preamble and the 32-bit tail. The preamble is used to detect the start of a burst, and determine the initial burst amplitude and decision threshold, whilst the tail is used to detect the end of a burst. For short packets such as 64 byte Ethernet packets of duration 57.6 ns at 10 Gb/s this would equate to a total overhead of 20%,

similar to that with 8B10B linecoding, however, for longer packets such as those proposed for OBS networks the overhead associated with the preamble and tail is minimal and the overhead is simply that of the eFEC (7.14%).

We have previously demonstrated the symbol timing recovery and dynamic range of this DBMRx without burst power equalization before the ADC [10]. The symbol timing recovery, necessary to recover the correct signal timing from the asynchronous samples, was shown to operate over a detuning range between the data rate and the sampling clock of  $\pm 14$  MHz at an input OSNR of 10 dB. The dynamic range of the DBMRx with respect to burst-to-burst power variations without automatic gain control was shown to be 7 dB. This dynamic range is limited at low burst amplitudes by the quantization error introduced by analogue to digital conversion process.

In order to improve the dynamic range of the receiver further it is necessary to employ automatic gain control (AGC) before the ADC to avoid the limitation arising from the quantization error that is introduced by the ADC stage. Burst equalization can be carried out either in the optical [11] or electrical domains. Here we investigate the performance and limitations of both electrical and optical burst equalization and demonstrate that the dynamic range can be dramatically increased by employing optical burst power equalization, using an electronically controlled SOA, before the receiver.

## 2. Digital burst-mode receiver implementation

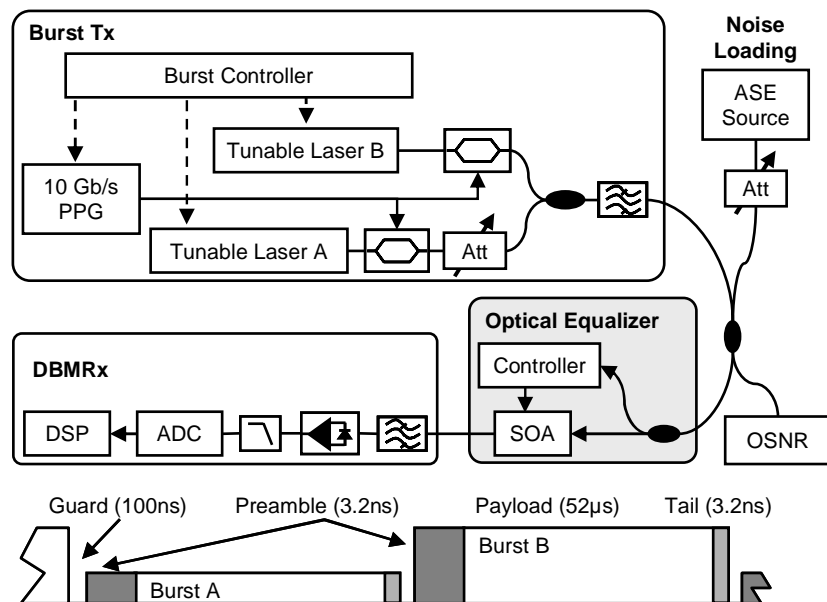


Fig. 1. Experimental burst transmitter, optical equaliser and digital burst-mode receiver. The burst structure is also shown.

The experimental set-up comprising optical burst transmitter, receiver and burst structure is shown in Fig. 1. The bursts are comprised of a 32-bit preamble of alternating ones and zeros, an arbitrary length data payload and optional address header. A 32-bit burst tail may also be used to facilitate the reception of bursts of an unknown length. The optical receiver consists of a 37.5 GHz Gaussian optical filter, standard 10 Gb/s AC-coupled pin pre-amp and an anti-aliasing filter. Digital sampling at twice the bitrate (20 GS/s) with an effective resolution of 5 bits was performed with a Tektronix TDS6154C real-time oscilloscope and is sufficient for all subsequent processing stages. The digital signal processing was carried out offline in MATLAB and the processing algorithm is shown schematically in Fig. 2.

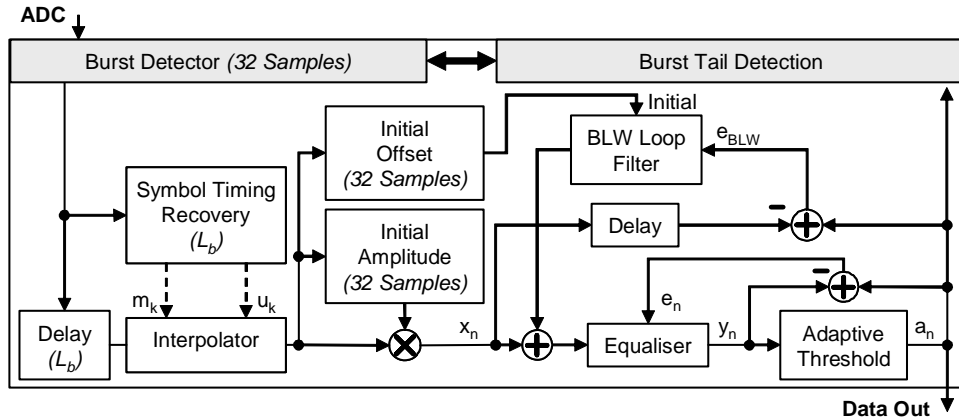


Fig. 2. Burst-mode receiver digital signal processing schematic.

Initially only the burst detector is active to detect a burst arrival over background noise. The burst detector comprises a 32 sample FIR digital correlator to detect the burst preamble and a decision circuit to indicate burst arrival. Once a burst is detected the burst detector is disabled and the rest of the system is enabled to recover the burst data.

The data recovery processing involves two stages. Firstly, timing recovery and interpolation are used to produce synchronized samples [9] and, secondly, amplitude and BLW corrections are applied before an adaptive decision circuit is used to recover the data.

The symbol timing recovery uses a feed-forward system based on two samples per symbol [12]. The requirement for only two samples per symbol is important as this allows for sampling at only twice the bit rate and minimizes the subsequent digital processing overhead. Feed-forward timing recovery is advantageous in a BMR to avoid the slow acquisition time found in feedback schemes. The timing recovery processes the samples in blocks of length ( $L_b$ ) and returns updated timing information at the block rate ( $1/L_b$ ). In this receiver the dynamic range of the timing recovery is inversely proportional to the block length, however, the resistance to noise is proportional to the block length, thus, there is a trade-off between these two requirements. Here we chose a block length of 512 samples in order to achieve a FEC error free performance of  $10^{-3}$  at an input OSNR of 10 dB when there was no frequency offset. With a block length of 512 samples, the interpolator timing information is updated at a rate of 39 MHz. The extracted timing information consists of the basepoint sample ( $m_k$ ) and a fractional interval ( $u_k$ ) which describes the point at which the interpolant should be calculated after the basepoint sample. To allow time for the symbol timing recovery the signal is delayed by the block length at the input to a simple linear interpolator implemented here as a two tap FIR filter with variable coefficients to produce two synchronised samples per symbol.

The initial burst amplitude, DC offset and decision threshold are calculated using the remaining 32 samples of the known preamble. This information is used to rescale the burst amplitude and correct for the initial DC offset that arises from the AC-coupling. The BLW correction is based on a data-aided technique [13] which makes use of an error signal ( $e_{BLW}$ ) generated by the difference between the recovered data ( $a_n$ ) and the uncompensated signal ( $x_n$ ) with an additional timing adjustment to compensate for equaliser delay. The design of the BLW loop filter is a trade-off between a sufficiently fast response time in adapting to the BLW caused by the AC-coupling and insensitivity to random noise. Averaging over 256 symbols was a good compromise to ensure operation at  $BER=10^{-3}$  for OSNR values around 10 dB.

Next, a 3-bit fractionally spaced adaptive feedforward equaliser is used to compensate for any remaining amplitude and phase fluctuations across the bursts. The equaliser, adapted using a decision-directed least mean squares algorithm, also downsamples the signal to one sample per symbol. A decision circuit with an adaptive threshold is then used to recover the

data. The use of an adaptive threshold is necessary to cope with the large dynamic range in power, OSNR and asymmetry in the noise distributions of the ones and zeros that the BMR must handle. We use a feedback threshold adaptation technique based on eye sampling using two subdecision levels to optimize the threshold [14].

A digital correlator is used to detect the reserved 32 bit burst tail sequence at which point the burst detector is re-enabled to detect subsequent bursts. The use of a tail sequence allows for variable length bursts, however, errors in the detection of the burst tail will propagate to subsequent bursts. In order to limit the range over which such errors can propagate a timeout is also used, however, this limits the maximum burst duration to less than the timeout which was set to 200  $\mu$ s in this work.

### 3. Experimental results and discussion

The DBMRx was characterized using the setup shown in Fig. 1. 10 Gb/s bursts were generated by two burst mode transmitters based on externally-modulated fast wavelength-tunable lasers. The driver limited switching time of these lasers set the minimum guard band between bursts to 100 ns. The burst duration was chosen to be 52  $\mu$ s as a compromise between improving the error statistics and reducing the offline processing time. The data payload consisted of 522144 bit  $2^{15}$ -1 PRBS NRZ data sequence.

Initially, in order to reduce complexity in the analogue domain and provide a baseline to compare performance against, no automatic gain control (AGC) was employed in the receiver design. Consequently, there is a penalty due to the quantization error of the ADC as the signal power is reduced. The dynamic range with respect to power variations between bursts of the receivers was evaluated by fixing the power incident on the receiver from burst B at -6 dBm and attenuating the power of burst A from -6 dBm down to -19 dBm. The receiver performance was quantified by optical noise loading at the receiver [15] to allow for error counting and the performance metric used is the required OSNR for a BER of  $10^{-3}$ . Direct counting of errors is used in this work because the more conventional gaussian extrapolation technique [16] based on the error free signal distributions is no longer valid after nonlinear digital signal processing. Here, we assume that enhanced Forward Error Correction (eFEC) would be used in this system and hence, these measurements are carried out using a pre-eFEC BER of  $10^{-3}$  as the reference point. An uncorrected BER of  $10^{-3}$  is correctable to better than  $10^{-15}$  with eFEC (ITU standard G.975.1) [17]. Figure 3 shows that the DBMRx without AGC provides a burst-to-burst dynamic range of 7 dB for a required OSNR penalty of less than 1 dB.

The performance of AGC was first investigated by placing a variable gain electrical amplifier between the photodiode and the ADC to perform burst by burst power equalisation. However, use of an AC-coupled receiver results in large BLW excursions of the initial part of the burst as shown on the input signal in Fig. 4(a). After amplification these excursions are clipped by the rails of the ADC which leads to loss of data from the start of the burst as shown in Fig. 4(b). Thus, it is necessary to use a DC-coupled amplifier to avoid clipping in the ADC. Such DC-coupled variable gain amplifiers at 10 Gb/s are not readily available so, to eliminate the effects of AC-coupling, both bursts were equally attenuated and the performance with and without AGC, using an AC-coupled variable gain amplifier, was measured. Figure 3 shows that without AGC the performance of the DBMRx with equal power bursts is similar to that obtained when the burst power varies from burst-to-burst. This indicates that the amplitude of the previous burst and hence the variation in the initial burst offset of the subsequent burst does not effect the performance of the DBMRx. This is consistent with Eldering's theoretical work on the sensitivity penalty of burst mode receivers which showed that for threshold determination based on a preamble of 16 or more bits the penalty when compared to continuous operation was less than 0.28 dB [18]. In this work a burst preamble of 16 bits is used to determine the initial amplitude and decision threshold. When AGC is employed the optical power margin is increased by 4 dB as shown in Fig. 3 and the receiver sensitivity is now limited by electrical noise arising from the photodiode and variable gain amplifier.

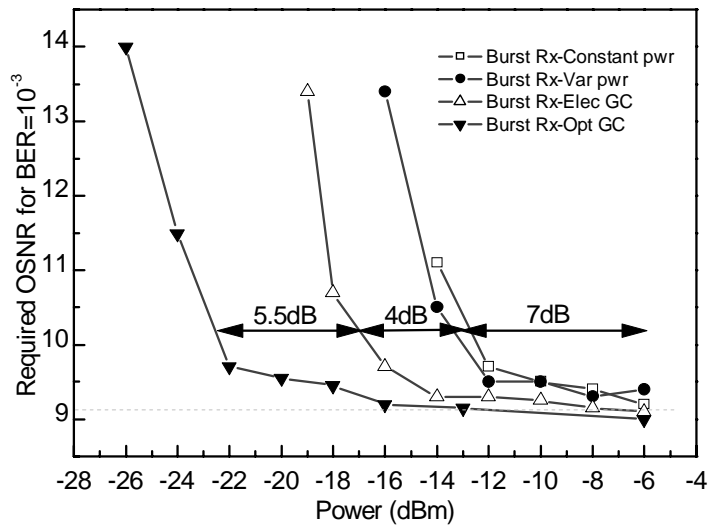


Fig. 3. The required OSNR for an error rate of  $10^{-3}$  as a function of the received power.

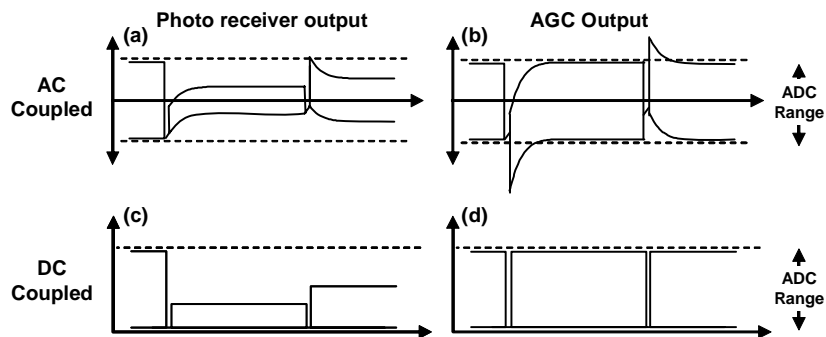


Fig. 4. An illustration showing the clipping that occurs, in the ADC, at the start of the burst signals when (a) an AC-coupled photo receiver followed by (b) an AC-coupled variable gain amplifier are used before the ADC. Also shown for comparison are the outputs of (c) a DC coupled photo receiver followed by (d) variable gain amplifier where clipping is avoided.

Secondly, we investigated optical burst power equalization before the photodiode using an electrically gain controlled SOA. The equalization of the burst power before the photodiode allows a conventional AC-coupled photodiode to be used as the effects of BLW are minimised and ensures that the full quantization range of the ADC is used for both weak and strong bursts, thus, reducing the penalty resulting from the quantization error. In an actual system the SOA gain would be set by a feed-forward controller based on a measurement of the average power of the incoming bursts such as that proposed by Aw et al. [19]. However, for the purposes of this demonstration where there are only two bursts of known amplitude we simply used an arbitrary waveform generator to supply the two level electrical drive signal that sets the SOA gain thereby equalizing the bursts. The SOA gain could be varied between transparency and 10.5 dB with a switching time of much less than the 100 ns guard time that was used in these experiments. Figure 3 shows that the use of optical burst equalization before the receiver improves the power margin by 9.5 dB from that obtained without any equalization. This increase in power margin is consistent with the variable gain provided by the SOA.

#### **4. Conclusions**

An AC-coupled digital burst-mode receiver for 10 Gb/s NRZ data, without additional line coding, suitable for use in OBS, OPS and PONs has been demonstrated. Asynchronous ADC at 20 GS/s allows for efficient implementation of symbol timing recovery, amplitude and baseline wander compensation in digital signal processing requiring only a 32 bit burst preamble. This is equivalent to a burst acquisition time of 3.2 ns. In addition to this overhead the use of eFEC will add a further 7.14% overhead. The receiver has a 7 dB burst-to-burst dynamic range with respect to burst power variations which is limited by the quantization error in the ADC.

The use of electrical gain control overcomes the limitations arising from the quantization error improving the dynamic range to 11 dB, however, this necessitates the use of a DC coupled photo receiver and variable gain amplifier. Optical burst equalization before the photo receiver and ADC overcomes the limitations arising from the quantization error without the need for a DC-coupled receiver and variable gain amplifier and further extends the dynamic range to 16.5 dB.

The low overhead, small penalty burst transmission, large dynamic range and burst length versatility make this type of receiver ideal for application in dynamic network architectures with burst timescales ranging from nanoseconds through to continuous data.

#### **Acknowledgments**

This work was supported by an EPSRC Advanced Research Fellowship EP/D074088/1, EU NOBEL, and Bookham Technologies.